Combustion Analysis and Devolatilazation kinetics of Gmelina, Mango, Neem and Tropical Almond Woods under Oxidative Condition

Edmund Okoroigwe‡,

National Centre for Energy Research and Development, University of Nigeria, Nsukka, Enugu State, Nigeria

‡ Corresponding Author; National Centre for Energy Research and Development, University of Nigeria, Nsukka, Enugu State, Nigeria, Tel: +234-8057156223, edmund.okoroigwe@unn.edu.ng

Received: 30.06.2015- Accepted:03.08.2015

Abstract- Thermogravimetric method was used to study the devolatilization characteristics and kinetics of Gmelina wood (*Gmelina arborea*), Mango wood (*Mangifera indica*), Neem wood (*Azadiracta indica*) and Tropical Almond wood (*Terminalia catappa*) under synthetic air condition at the heating rate of 30^{o}C/min. It was observed that all the samples followed a two-stage reaction mechanism between 200^{o}C and 500^{o}C clearly indicating regions of volatile oxidation and char combustion. The maximum rate of weight loss (%/^{o}C) are 2.20, 1.50, 1.25 and 1.60 for Gmelina wood, Mango wood, Neem wood and Tropical almond wood respectively and occurred at peak temperatures of 310^{o}C, 322^{o}C, 320^{o}C and 320^{o}C in the same order of sample presentation. During the oxidative stage, the activation energy of the samples, based on the Arrhenius correlation are 125,108, 142 and 113 KJ/mol respectively while during the char combustion stage the activation energy are 257, 210, 281 and 345 KJ/mol in that same order. This shows that the samples would require less energy input for their thermochemical conversion to bioenergy and would not pose any barrier to their use in combustion reactors. The samples are thus good potential feedstock among the league of biomass resources for present and future bioenergy fuels.

Keywords- Biomass, Thermogravimetric analysis, combustion, kinetic study, activation energy, reaction order.

1. Introduction

Conversion of biomass to energy has gained global recognition in recent times, through research and development, as a way to solving world's energy problems and climate change abatement. Many countries of the world are working assiduously towards integrating biomass energy resources into their national energy mix through meaningful renewable energy polices. An example is the UK's target of 20% replacement of fossil fuel usage with renewable energy alternatives by 2020 [1] with biomass playing a major role. Thermo-chemical and bio-chemical processes are established ways of converting biomass to energy with the former dominating due to its higher conversion efficiency status in production of gaseous, liquid and solid fuels [2,3]. Biomass, even though is globally wide spread, it is still environment specific. This is due to the fact that vegetation characteristics (type and nature of plants that grow therein) are climate dependent. The biomass feedstock resource present and available in any region may not be present and available in its natural form in another location. This raises concerns when transportation and feedstock costs logistics such as availability and sustainability would have to be considered for onsite energy production. For instance growing and processing energy crops (feedstock), which thrive favourably in Europe, will not pose much financial threats if they are to sustain power plants in Europe. It becomes an issue if such feedstock would be transported to any other continent for the same purpose. First, the concern of cost of feedstock and its transportation handling logistics come into play. Secondly, feedstock security at the source might have to be considered. These altogether are the present features of conventional fossil fuels. Hence there is need to screen diverse wood biomass that could be potential feedstock for bioenergy production through combustion, gasification, torrefaction and fast pyrolysis. By this, the fear of regionalized biomass unavailability and cost will be eliminated.

Even though there is significant research in biomass to energy conversion activities involving several biomass species, there is insignificant information on the thermal characteristics of Gmelina, Mango, Neem and Tropical Almond woods. Development of thermal conversion processes, such as combustion, torrefaction, gasification and pyrolysis, based on these samples, require a good understanding of their thermal characteristics. This work aims at determining the thermal conversion characteristics of the samples under combustion condition. These will aid in determining the potential of these samples to serve as bioenergy production resources for the regions where they are grown and for the entire biomass world industry.

A good amount of work has been done in determining these characteristics using different biomass materials under inert (pyrolysis) condition [2, 4 – 12]. Similarly, under oxidative conditions, some scholars have carried out research to determine the aforementioned characteristics of different biomass species [3,13 – 19].

Gmelina wood is a household name in wood and forest industry in Nigeria while Mango wood is a common cash crop in Nigeria's agricultural industry which produces large residue. Neem plant leaves are medicinal while the tree itself and the Tropical Almond tree are ornamental plants that thrive well in tropical Nigeria. Due to their abundance, residues from them constitute environmental nuisance if not disposed. Currently, burning is the only way to reduce or eliminate them where they occur due to lack of adequate and better alternative to their use. Harnessing the bioenergy potential of these biomass species will help to expand the global biomass and biofuel production market and aiding in solving Nigeria's and global energy problems in addition. The knowledge of their combustion kinetics is important for proper design of a combustion reactor which plays an important role in large-scale combustion process. The combustion kinetics can be studied by several methods but the most popular and simplest technique is the thermogravimetric analysis (TGA). Hence the objective of this work is to generate the thermal decomposition parameters (data) of the four tropical biomass species through thermogravimetric analysis and to investigate their suitability for bioenergy production purposes.

2. Experimental

In this work, four woody biomass samples viz: Gmelina wood (*Gmelina arborea*), Mango wood (*Mangifera indica)*, Neem wood (*Azadiracta indica*) and Tropical Almond wood (*Terminalia catappa*) were selected for study. These fall within agricultural and forestry residues. The feedstock samples were obtained within Nsukka urban and milled to about 1mm particle size using Wiley milling machine. The samples were first characterized to determine their proximate and ultimate parameters, heating values, structural carbohydrate composition. The non-isothermal TGA study was carried out using Thermogravimetric instruments TGA Q500 system at temperature range of 30^{o}C to 750^{o}C under synthetic air at a temperature gradient of 30^{o}C/min. Sample masses of 32.2710, 15.0070, 19.0940 and 18.7920mg of gmelina wood, mango wood, neem wood and tropical almond wood were used respectively. Higher heating rate corresponding to the large sample mass was to reduce the effects of heat and mass transfer on the results. Decomposition of biomass by combustion is a complex phenomenon due to differences in chemical composition of the structural components of the biomass [3]. Because of this it will be difficult and indeed erroneous to use a single kinetic model to explain the decomposition process involving several biomasses. Therefore, in this work the popular Arrhenius equation which is used by many scholars is employed in the determination of the kinetic parameters [3, 6,11,12,14 – 16, 20, 21]. The kinetic reaction parameters of the feedstock such as activation energy, pre-exponential factors and reaction orders, were determined using the data generated from the TG-DTG experiment by application of SCILAB software version 5.4.1

3. Results and Discussion

3.1 Oxidative thermal characteristics of the samples

Combustion of any fuel (biomass) usually takes place whenever oxygen comes in contact with the fuel and can take place at any temperature. The TG and the corresponding DTG curves are shown in Figs. 1a – 1d for each sample following the sequence above while Figs. 2 and 3 respectively show the TGA and DTG curves of all the samples together.

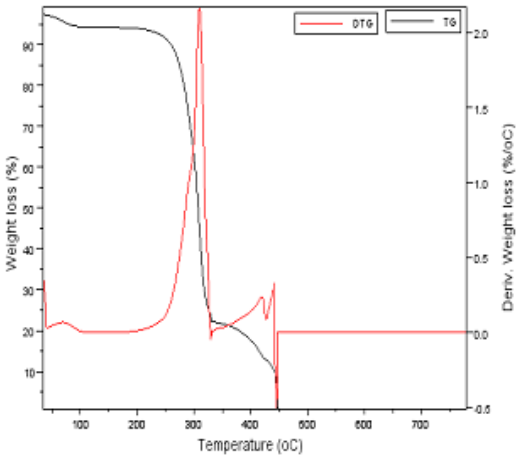

a): Gmelina wood.

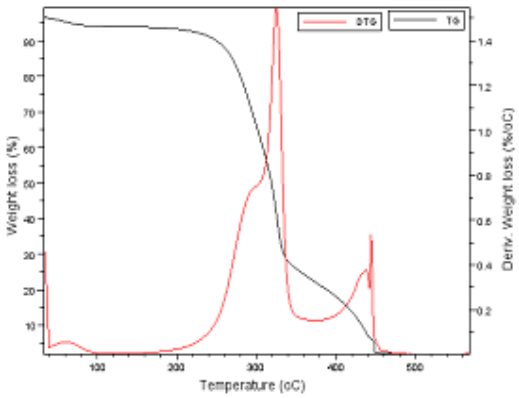

b): Mango wood

.

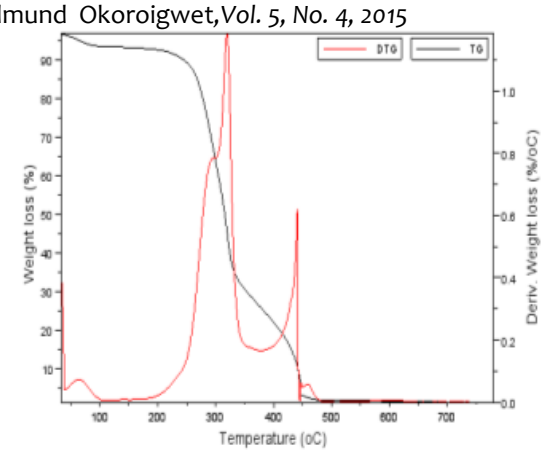

c): Neem wood

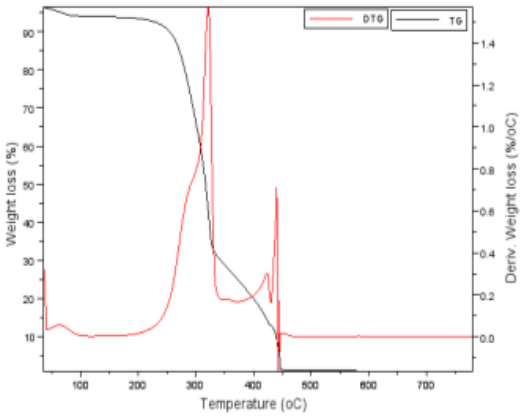

d): Tropical Almond wood

Figure 1. TG and DTG of different samples

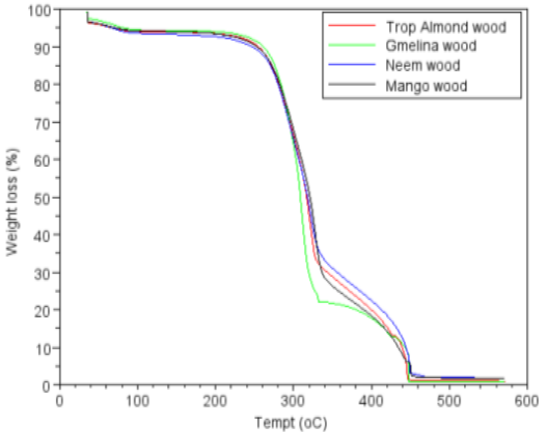

Figure 2. TG plots of all sample

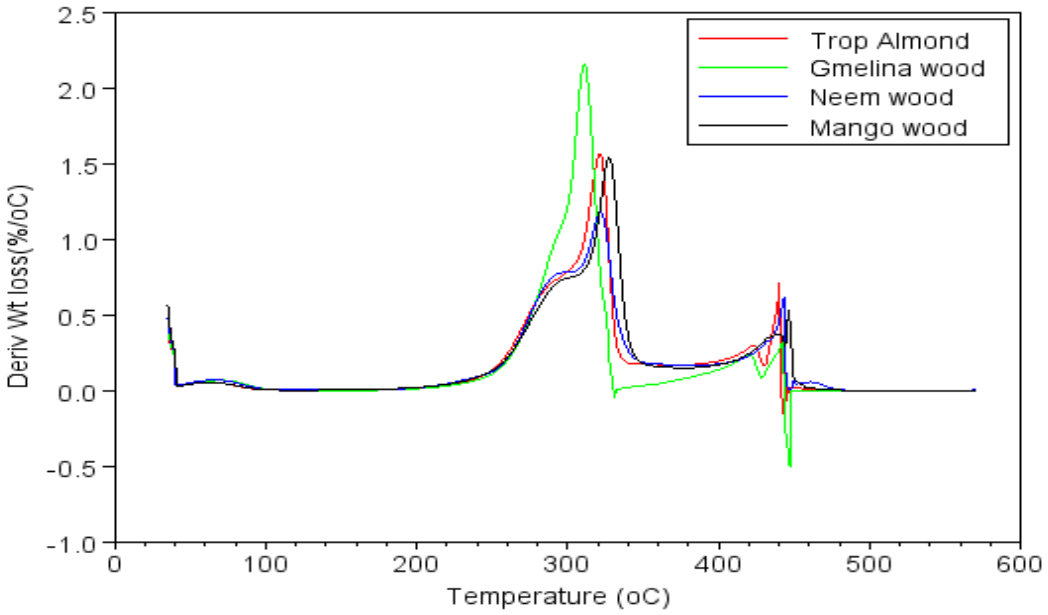

Figure 3. DTG plots of all samples

Table 1. Characteristics of oxidative thermogravimetric analysis of the samples

Biomass (wood sample)		Oxidative degradation zone					Char combustion zone				
	Moisture loss (%)	T_{peak} (°C)	Volatiles (%)	Temperature range (°C)	Max weight loss rate (%/°C)	Average weight loss rate R_a (%/°C)	Temperature range (°C)	R_{max} (%/°C)	Ave rate (%/°C)	R_M x10^3 (%/°Cs^{-1})	Ash (%)
Gmelina	7.0	310	85.0	210 - 330	2.20	0.5665	330 - 480	0.40	0.0726	1.02	8.0
Mango	6.5	322	89.0	210 -350	1.50	0.4766	390 - 480	0.55	0.1744	0.48	4.5
Neem	7.0	320	89.0	210 -350	1.25	0.4380	390 - 480	0.65	0.1668	0.41	4.0
Tropicalalmond	7.0	320	87.0	210 -350	1.60	0.4582	390 - 480	0.75	0.1447	0.48	6.0

Table 1 shows the summary of the thermogravimetric characteristics of the studied samples under synthetic air condition. It is evident from the curves that the decomposition process of the samples under synthetic air demonstrated a three stage weight loss similar to the decomposition of samples used by reference [3] and reference [15]. The first stage is the moisture evaporation (30 – 100°C), the second stage from 200 to 350°C (Table 1), depending on the biomass, is the devolatilization of volatiles or decomposition of structural carbohydrates – hemicelluloses, celluloses and light lignin and the last stage of weight loss shows the combustion of char (350 - 500°C).

The DTG curve in Figure 3 shows the reaction/decomposition rate as a function of temperature represented by the height of the plots. The reactivity of the combustion regions is proportional to the height of the DTG peak [13]. Similarly, the temperature at which this occurs is also a measure of the reactivity of the samples [19]. Therefore, in this work gmelina wood is the most reactive while tropical almond wood and mango wood had similar reaction rate. The least reactive biomass among the samples is neem wood. The maximum rate of weight loss (%/°C) at peak temperature of 310°C, 322°C, 320°C and 320°C were 2.20, 1.50, 1.25 and 1.60 in the same order of sample presentation. It is in this region that volatiles are released and burned [19]. Furthermore, in this region the peak temperatures associated with the devolatilization of the volatiles are obtained.

This temperature is significant in the design of thermal conversion processes and reactors. The average weight loss rate presented in Table 1 shows that gmelina wood had the highest average weight loss rate of 0.5665%/°C followed by mango wood = 0.4766, then tropical almond wood 0.4582%/°C and the least is neem wood 0.4380%/°C. It is explained that at this stage of structural carbohydrate devolatlization, porosity of char increases causing oxygen diffusion into the particles hence increase in combustion rate [3,22]. It is also in this range of temperature that burning takes place due to release of volatiles [19].

From Figure 2 and 3, it follows that the end of stage 2 begins the char combustion stage. This takes place within the temperature ranges stated in Table 1 for different biomass species used. In the case of gmelina wood, the char combustion overlapped the volatiles degradation at 330°C while the rest began at temperature of 390°C after the volatile degradation ended at 350°C.

The four samples have similar char combustion profiles showing two stages of decomposition. Gmelina and Almond wood have the same first peak temperature at 422°C. The second char combustion peak temperature of tropical almond wood corresponds to the first char combustion peak temperature of mango wood at 440°C. Similarly, the first char combustion peak temperature of neem wood corresponds to the second peak temperature of gmelina wood at 442°C. The second peak temperature of mango wood is 444°C while the second peak temperature of neem wood is 462°C. The similarity of two stage combustion process suggests that the biomass materials have similar chemical components that make up the nature of the materials and also two different char components taking part in the reaction [3]. Another insight from this experience is that the design of thermochemical processes involving these samples may not vary significantly. It is observed from Figure 2b and Table 1 that the average weight loss (%/°C) of the char combustion region is less than that for burning region in all the samples. This is not surprise because at this region only lignin decomposes while at the burning region both hemicelluloses and cellulose are burnt and it is in the later structures that most volatiles are contained.

3.2. Reactivity, ignition and combustion index

The reactivity of samples under inert and oxidative conditions has been defined previously [3, 15, 23, 24]. Reactivity R_M is directly proportional to the maximum weight loss rate R_{DTGmax} and inversely proportional to its corresponding peak temperature T_P. Hence

$$R_M = 100 \sum \frac{R_{DTGmax}}{T_{DTGmax}} \quad (1)$$

The summation takes account of any secondary peak or shoulder present in the burning region. The summary of the calculated reactivity based on peak weight loss, peak temperature and time of occurrence for all the samples under burning region is presented in Table1. *Note: peak temperature T_p in table is same as denominator of eqn (1), which shows the temperature corresponding to the maximum peak on the DTG curve*. Based on this gmelina wood appear

to be most reactive because its cellulose and hemicelluloses decomposition took place at the same temperature and time resulting in only one peak. The rest of the samples had secondary peaks on DTG curve showing close decomposition temperature of both cellulose and hemicelluloses. Based on this also reactivity of the samples can be ranked from the most reactive to least reactive thus: gmelina > mango = tropical almond > neem wood. The values are less than those presented by [15] for date palm waste except for gmelina wood.

It has been shown also that the reactivity of carbonaceous materials under oxidative conditions is proportional to the cellulose content of the feedstock [24]. The result obtained in this work agrees with this theory. Since both cellulose and the hemicelluloses take part in the burning stage, the reactivity correlates with these structures as shown in Table 2. Hence we can rank the samples in decreasing order of reactivity thus gmelina > mango > neem > tropical almond wood.

Table 2. Structural carbohydrate and lignin content of samples

Biomass	Lignin	Cellulose	Hemicellulose	Inorganic materials
Gmelinawood	25.83	42.79	16.98	14.4
Mango wood	22.67	43.72	14.48	19.13
Neemwood	26.51	38.89	15.82	18.78
Tropicalalmondwood	27.78	41.78	9.81	20.63

Table 3. Combustion characteristics of the samples

Sample	Ti	t_i (s)	R_a	Rmax	t_{max} (s)	T_b (°C)	t_b(s)	D x10^8	S x10^9
Gmelinawood	290	2241	0.5665	0.40	3058	450	3220	5.8368	5.9875
Mango wood	275	2175	0.4766	0.55	3173	450	3236	7.9695	7.7026
Neemwood	260	2090	0.4380	0.65	3141	465	3317	9.9015	9.0571
TropicalAlmondwood	270	2135	0.4582	0.70	3087	450	3212	10.621	9.7772

3.3. Ignition and burn-out temperature

Other important combustion characteristics of biomass materials worth noting in this work are the initial ignition temperature and the burnout temperature. These are associated with combustion and ignition indices of the substances. Ignition temperature T_i and burn out temperature T_b are as defined by [15, 16, 25].

The ignition index D_i and combustion index S are calculated by equations 2 and 3 according to methods used by other authors [15, 16, 25, 26] in previous research involving other biomass samples

$$D_i = \frac{R_{max}}{t_m t_i} \quad (2)$$

$$S = \frac{R_{max} R_a}{T_i^2 T_b} \quad (3)$$

Where R_{max} is the maximum combustion rate (%/°C),

t_m and $t_i$are times corresponding to maximum combustion rate and ignition temperature respectively. R_a is the average mass loss rate.

The ignition temperature of the samples is shown in Table 3 with the corresponding times to ignite. It shows that neem wood has the least ignition temperature as well as the early burning time while gmelina wood has the largest ignition temperature and the corresponding burning time.

The values obtained for these tropical biomass samples are larger than those of date palm residues from arid region North Africa [15]. Similarly, the ignition and combustion indices of the samples studied in this work are greater than those presented by [16] for sewage sludge. This is expected because of the high moisture content expected in sewage sludge. As expected for fossil fuels, the ignition characteristics of coal, its blends and waste tyres studied by ref [25] are better than those of the samples in this work. This is because of the low hydrocarbon content associated with biomass materials. The burnout temperatures are similar in all the samples except neem wood even though it has the smallest ignition temperature. Even though the difference in the burn out temperature of neem wood is relatively small, it could be that the biomass contains more difficult-to-combust lignin materials than the rest. This also shows that these biomass samples can be converted to bioenergy with similar reactor without much design adjustment.

3.4. Kinetic studies

The multiple peaks on the DTG curves show that the decomposition of the structural carbohydrates and lignin in the samples under consideration follow two stage reaction schemes. The first stage is the oxidation of hemicelluloses and cellulose or combustion of volatiles while the second stage is the combustion of char formed during the 1st stage and the remaining lignin [11]. All models used for biomass kinetic studies are based on rate laws that obey Arrhenius rate expression:

$k(T) = Ae^{-E/RT}$ (4)

where:

k(T) is temperature dependent reaction rate constant,
A is pre-exponential or frequency factor,
E is activation energy (J/mol)
R is universal gas constant = 8.314J/mol.K
T is absolute temperature, K

The activation energy is regarded as "the energy threshold that must be overcome before molecules can get close enough to react and form products" [12].

The kinetics of biomass decomposition and other combustible materials can be expressed by the relation

$\frac{d\alpha}{dt} = k(T)f(\alpha) = Ae^{-E/RT}$ f(α) (5)

Where t is time, α is degree of conversion, dα/dt is rate of isothermal process and f(α) is the conversion function that represents the model used which depends on the controlling mechanism.

$f(\alpha) = (1-\alpha)^n$ (6)

By definition α can be expressed as the mass fraction of biomass substrate that has decomposed in a time t during the decomposition process or mass fraction of volatiles evolved [12].

Hence $\alpha = \frac{m_{o-m}}{m_{o-m_f}}$ (7),

Where m_o, is the mass of the biomass substrate at the beginning of reaction, *m* is the mass of the biomass substrate at anytime *t* and m_f, is the mass of the biomass at the end of the reaction time. The unreacted mass or residue is accounted for in m_f.

For non-isothermal decomposition, the rate expression which represents reaction rates as function of temperature at a linear heating rate is:

$\frac{d\alpha}{dT} = \frac{d\alpha}{dt}\frac{dt}{dT}$ (8)

Where $\frac{d\alpha}{dT}$ is the non-isothermal reaction rate, $\frac{d\alpha}{dt}$ is the isothermal reaction rate and $\frac{dt}{dT}$ is the reciprocal of heating rate (γ^{-1}). Since the isothermal rate is defined in equation 4, then the non-isothermal rate can be expressed by substituting this in equation 8, thus

$\frac{d\alpha}{dT} = \frac{A}{\gamma}e^{-E/RT}$ f(α) (9).

In solving equation 9, the Coats-Redfern [27] method is used because it is the popular non-isothermal model fitting method used for the determination of the reaction processes [7, 11, 12, 20, 21].

Integratingbothsides of equation 9,

$\int \frac{d\alpha}{f(\alpha)} = \frac{A}{\gamma}\int exp(-\frac{E}{RT})\,dT,$

we have the general solution

$g(\alpha) = \int_0^\alpha \frac{d(\alpha)}{f(\alpha)} = \frac{A}{\gamma}\int_{T_0}^{T} \exp(-\frac{E}{RT})dT$ (10)

It has become difficult for scholars who are new to this method to understand the process of solving this relationship. Hence in this work it is intended to provide details of its relationship.

See appendix A for details

The general method as adopted in the pseudo component model for obtaining the kinetic parameters (E, A and n) and determining the form of g(α) is byplotting the mass loss data from Thermogravimetric Analysis (TGA) with temperature. A plot of $ln\left[\frac{g(\alpha)}{T^2}\right]$ against T^{-1} is a straight line whose slope is $-\frac{E}{R}$andtheintercept is $ln\left[\frac{AR}{\gamma E}\right]$. From these, both E and A can be estimated. Negative form of $ln\left[\frac{g(\alpha)}{T^2}\right]$ can be plotted against reciprocal of T to obtain

E/R as slope and negative $ln\left[\frac{AR}{\gamma E}\right]$as intercept. The regression analyses of the TGA data were carried out using LINREGR tools of SCILAB software. Equation 20 was plotted for the two stages of devolatilization. Different reaction orders, n (0 – 3) were substituted in g(α) to obtain different forms of g(α) The reaction order corresponding to the highest correlation factor R^2 for any stage is taken to govern the decomposition of the sample within that stage. Plots of $-ln\left[\frac{g(\alpha)}{T^2}\right]$against T^{-1} forburningandcharcombustionstages of thesamplesareshown in Figs. 4 and 5. The slope and the intercepts of the plots were used to estimate the activation energies and pre-exponential factors of the samples. Tables 4 and 5 show the summary of the estimated correlation factors R^2, activation energy E and pre-exponential factor A, for the burning and char combustion stages respectively.

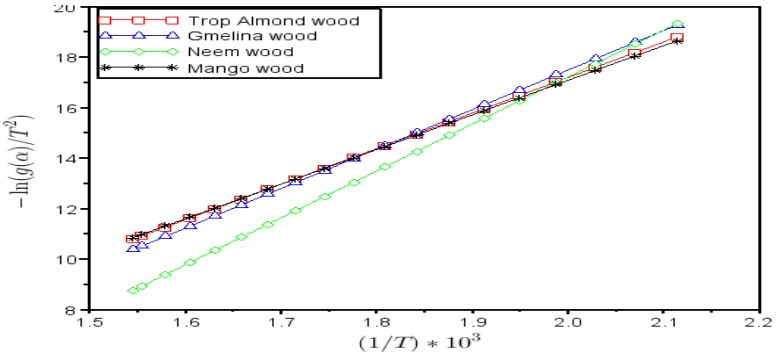

Figure 4. Plot of $-\ln\left[\frac{g(\alpha)}{T^2}\right]$ against T^{-1} for all samples during oxidation stage

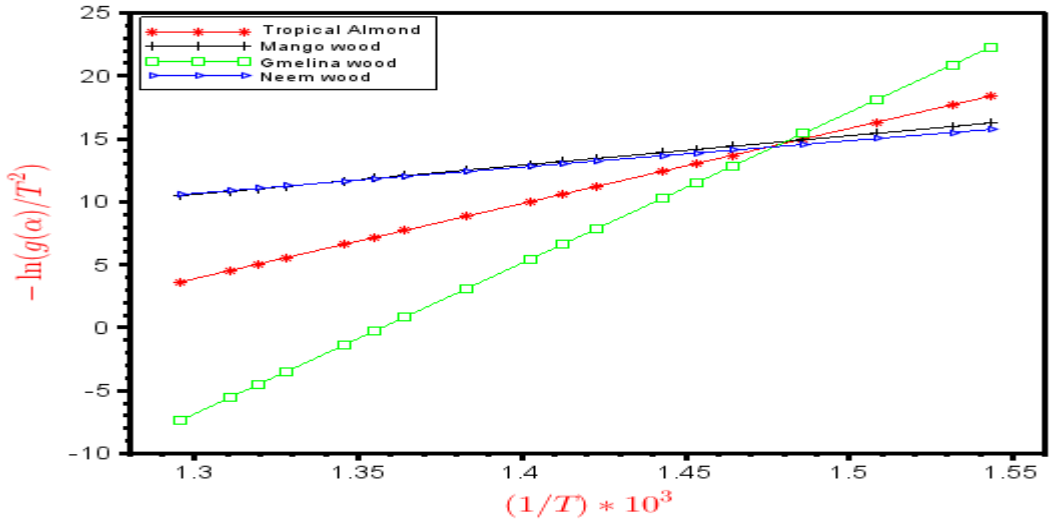

Fig. 5. Plot of $-\ln\left[\frac{g(\alpha)}{T^2}\right]$ against T^{-1} for all samples during char combustion

Table 4. Summary of the estimated kinetic parameters for oxidation stage

Sample	Factor of correlation, R^2				Reaction kinetic parameters		
	Reaction order, n				Determined reaction order	Activation energy, E	Frequency factor, A
	0	1	2	3	n	(KJ/mol)	(min^{-1})
Gmelinawood	0.9249787	0.9778686	0.9714073	0.9193204	1	125.11334	11645.523
Mango wood	0.9311404	0.9834147	0.9712147	0.9096674	1	107.86641	8686.2965
Neemwood	0.9163795	0.9766171	0.980467	0.9318465	2	142.08054	14740.358
Almondwood	0.9272581	0.9809919	0.9817636	0.9325791	1	112.74785	9512.4385

Table 5. Summary of the estimated kinetic reaction parameters for Char combustion stage

Sample	Factor of correlation, R^2				Reaction kinetic parameters		
	Reaction order, n				Determined reaction order	Activation energy, E	Frequency factor, A
	0	1	2	3	n	(KJ/mol)	(min^{-1})
Gmelinawood	0.8547994	0.8903890	0.920218	0.9432331	3	256.50576	32051.531
Mango wood	0.8777241	0.9277918	0.8142362	0.6740985	1	210.48197	24008.275
Neemwood	0.8618220	0.9274585	0.9402322	0.9110246	2	280.97448	36695.16
Almondwood	0.8493476	0.9389003	0.9625831	0.9383661	2	344.52066	48576.944

3.5 Activation energy

It can be observed from Table 4 that during the volatile oxidation stage, neem wood had the highest activation energy of 142.1KJ/mol while mango wood had the least activation energy of 107.9KJ/mol. Tropical almond wood's activation energy at this stage is slightly above that of mango wood while gmelina wood had an activation energy of 125.1KJ/mol. The implication here is that it would require lesser energy to decompose mango wood compared to the rest wood samples while at this stage, greater energy would be required for the conversion of neem wood to energy than others. It is also observed from Table 5 also that as decomposition temperature progressed to char region (350 – 500^{o}C), Tropical almond wood had the highest activation energy of 344.5KJ/mol and mango wood maintained the least activation energy of 210.5KJ/mol. Gmelina wood activation energy becomes 256.5KJ/mol while that of neem wood was 280.9KJ/mol. There is deficient information in literature on the activation energy of the studied biomass samples. However, it can be compared with those of other biomass studied under the same oxidative conditions. The activation energy of the samples under this study are higher than those presented by ref [3] for cotton stalk, sugar cane bagasse and shea meal. Variation in heating rate and other chemical composition differences in biomass samples can affect the activation energy significantly.

4 . Conclusion

The decomposition characteristics of the studied biomass samples under controlled synthetic air are established in this study. Data representing their thermal behavoiur during combustion processes are generated and presented. Two stage decomposition processes are followed by all the samples. The volatile oxidation stage was more critical in the samples since greater mass loss was recorded within this stage. The samples have very close combustion characteristics to each other such that similar reactors or combustors can be used to convert them to bioenergy without any adjustment in the design of the reaction system. Similarly at the heating rate of 30^{o}C/min, the average activation energy of the four samples ranged from 159 – 229KJ/mol which are suitable for thermal conversion to energy without much energy input. The samples possess good properties that make them potential feedstock for bioenergy production and utilization in combustion reactors.

References

[1] P. M. Connor, "UK renewable energy policy: a review", Renew. Sust. Energy Reviews vol. **7**, pp 65-82, February 2003.

[2] X. Zhang, M. Xu, R. Sun, and L. Sun, "Study on biomass pyrolysis kinetics", J Eng. Gas Turbines and Power, vol. 128 (3), pp 493-496, March 2004, doi: doi:10.1115/1.2135816

[3] S. Munir, S. S. Daood, W. Nimmo, A. M. Cunliffe, and B.M Gibbs "Thermal analysis and devolatilization kinetics of cotton stalk, sugar cane bagasse and shea meal under nitrogen and air atmospheres", Bioresour Technol. Vol.100 (3), 1413-1418, February 2009. doi:10.1016/j.biortech.2008.07.065

[4] K.G. Mansaray, and A. E. Ghaly, "Determination of reaction kinetics of rice husks in air using thermogravimetric analysis", Energy Sources vol.21 (10), 899-911, 1999 DOI**:**10.1080/00908319950014272

[5] M.G. Gronli, G. Varhegyi, and C. D. Blasi, "Thermogravimetric analysis and devolatilization kinetics of wood", Ind. Eng. Chem. Res. vol.41 (17), pp 4201-4208, July 2002.DOI: 10.1021/ie0201157

[6] A. J. Tsamba, W. Yang, and W. Blasiak, "Pyrolysis Characteristics and Global Kinetics of Coconut and Cashew nut shells". Fuel Proc. Technol. vol. 87 (6), pp 523-530, June 2006. doi:10.1016/j.fuproc.2005.12.002

[7] A. A. Zabaniotou, E. K. Kantarelis, and D. C. Theodoropoulos, "Sunflower shell utilization for energetic purposes in an integrated approach of energy crops: laboratory study pyrolysis and kinetics", Bioresour. Technol. vol. 99 (8), pp 3174-3181, May 2008. doi:10.1016/j.biortech.2007.05.060

[8] P.Luangkiattikhun, C. Tangsathitkulchai, and M. Tangsathitkulchai, "Non-isothermal thermogravimetric analysis of oil-palm solid wastes". Bioresour. Technol vol.99(5), pp 986-997, March 2008

[9] W. H. Chen, and P. C. Kuo, "A study on torrefaction of various biomass materials and its impact on

lignocellulosic structure simulated by a thermogravimetry", Energy vol. 35 (6), pp2580-2586, June 2010. doi:10.1016/j.energy.2010.02.054

[10] S. S. Idris, N. A. Rahman, K. Ismail, A. B. Alias, Z. A. Rashid, M. J. Aris, "Investigation on thermochemical behaviour of low rank Malaysian coal, oil palm biomass and their blends during pyrolysis via thermogravimetric analysis (TGA)". Bioresour Technol., vol.101 (12), pp 4584- 4592, June 2010.

[11] L. Wilson, W. Yang, W. Blasiak, G. R. John, and C. F. Mhilu, "Thermal characterization of tropical biomass feedstocks". Energy Conv. Mgmt. vol. 52 (1), pp191-198 January 2011. doi:10.1016/j.enconman.2010.06.058

[12] E. J. White, W. J. Catallo, and B. L. Legendre, "Biomass Pyrolysis Kinetics: a comparative critical review with relevant agricultural residue case studies", J. Anal. Appl. Pyrolysis vol. 91 (1**)**, pp1-33 May 2011. doi:10.1016/j.jaap.2011.01.004

[13] M. V. Kok, and E. Özgür "Thermal analysis and kinetics of biomass samples". Fuel Proc. Technol. vol. 106, pp739-743 February 2013. doi:10.1016/j.fuproc.2012.10.010

[14] H. H. Sait, H. Ahmad, A. S. Arshad, and N. A. Farid, "Pyrolysis and combustion kinetics of date palm biomass using thermogravimetric analysis". Bioresour Technol. vol.118, pp382-389, August 2012. http://dx.doi.org/10.1016/j.biortech.2012.04.081

[15] Y. El may, J. Mejdi, D. Sophie, T. Gwenaelle, and S. Rachid, S. "Study on the thermal behavior of different date palm residues: Characterization and devolatilization kinetics under inert and oxidative atmospheres". Energy, vol 44 (1), pp702-709, August 2012. doi:10.1016/j.energy.2012.05.022

[16] D. Vamvuka, and S. Sfakiotakis, "Combustion behaviour of biomass fuels and their blends with lignite" Thermochimica Acta, vol. 526 (1-2), pp192-199, November 2011. doi:10.1016/j.tca.2011.09.021

[17] O. Senneca, "Kinetics of pyrolysis, combustion and gasification of three biomass fuels". Fuel Proc. Technology, vol. 88 (1), pp87-97, January 2007. doi:10.1016/j.fuproc.2006.09.002

[18] I. Simkovic, and K. Csomorova, "Thermogravimetric analysis of agricultural residues: oxygen effect and environmental impact" J. Appl. Polymer Sc; vol.100 (2), 1318-1322, January 2006. DOI: 10.1002/app.23818

[19] H. Haykiri-Acma, "Combustion characteristics of different biomass materials". Energy Conv. Mgmt. vol.44 (1), pp155-162, January 2003. PII: S 01 9 6 - 8 9 04 (01) 002 00-X

[20] D. K. Shen, S. Gu, K. H. Luo, A. V. Bridgwater, and M. X. Fang, "Kinetic study on thermal decomposition of woods in oxidative environment". Fuel vol.88 (6), pp1024-1030, June 2009. doi:10.1016/j.fuel.2008.10.034

[21] A. Aboulkas, K. El harfi, and A. El Bouadili, "Thermal degradation behaviors of polyethylene and polypropylene. Part I: Pyrolysis kinetics and mechanisms". Energy Conv. Mgmt. vol.51 (7) pp1363-1369, July2010. doi:10.1016/j.enconman.2009.12.017

[22] A. Gani, and I Naruse, "Effect of cellulose and lignin content on pyrolysis and combustion characteristics for several types of biomass". Renew. Energy, vol.32 (4), pp649-661, April 2007. doi:10.1016/j.renene.2006.02.017

[23] S. W. Park, and C. H. Jang "Effects of pyrolysis temperature on changes in fuel characteristics of biomass char". Energy vol.39(1), pp187-195, March 2012. doi:10.1016/j.energy.2012.01.031

[24] P. Ghetti, R. Leandro, A. Luciana, "Thermal analysis of biomass and corresponding pyrolysis products". Fuel vol.**75** (5), pp565-573, April 1996. 0016-2361(95)00296-0

[25] L. Xiang-guo, M. Bao-guo, X. Li, H. Zhen-wu, and W. Xin-gang, "Thermogravimetric analysis of the co-combustion of the blends with high ash coal and waste tyres". Thermochimica Acta 441 (1), pp79-83, February 2006. doi:10.1016/j.tca.2005.11.044

[26] S. G. Sahu, P. Sarkar, N. Chakraborty, A. K. Adak, "Thermogravimetric assessment of combustion characteristics of blends of a coal with different biomass chars", Fuel Proc. Technology 91(3), pp369-378, March 2010. doi:10.1016/j.fuproc.2009.12.001

[27] A. W Coats, J. P.Redfern,"Kinetic parameters from thermogravimetric data". Nature vol. 20168 – 69, January 1964. doi:10.1038/201068a0

[28] E. D. Rainville, *Special functions*. Macmillan Company, New York, 1960, pp22 &44

Appendix A

Equation 10, can be solved as

$$\int_0^{\alpha} \frac{d(\alpha)}{(1-\alpha)^n} = \frac{A}{\gamma}\int_{T_0}^{T} \exp(-\frac{E}{RT})dT$$

Integrating the left hand side first,

$g(\alpha) = \int_o^{\propto} \frac{d(\alpha)}{(1-\alpha)^n}$,

If n = 1, then,

$$g(\alpha) = \int_o^{\alpha} \frac{d(\alpha)}{(1-\alpha)}$$

$$= [-ln(1-\alpha)] - 0$$

$$= -ln(1-\alpha) \qquad (11a)$$

If $n \neq 1$, then, $g(\alpha) = \int_o^{\alpha} \frac{d(\alpha)}{(1-\alpha)^n}$

$$= \left[\frac{(1-\alpha)^{-n+1}}{-n+1}\right]_0^{\alpha}$$

$$= \left[\frac{-(1-\alpha)^{1-n}}{1-n}\right] - \left[\frac{-(1)^{1-n}}{1-n}\right]$$

$$= \frac{1}{1-n} - \frac{(1-\alpha)^{1-n}}{1-n}$$

$= \frac{1-(1-\alpha)^{1-n}}{1-n}$ (11b)

The RHS of equation 11 is thus

$F(T) = \frac{A}{\gamma}\int_{T_0}^{T} exp(-\frac{E}{RT})dT.$

This can be solved by making the substitution, $X = \frac{E}{RT}$ (12)

Hence, $\frac{dX}{dT} = \frac{-E}{RT^2}$, $dT = \frac{-RT^2}{E}dX$, $X^2 = \frac{E^2}{(RT)^2}$ and $\frac{RT^2}{E} = \frac{E}{RX^2}$

from équation (11), T → 0, X →∞ , T → T, X → X.

$$\therefore F(T) = \frac{A}{\gamma}\int exp\left(-\frac{E}{RT}\right)dT$$

$F(X) = \frac{A}{\gamma}\int_{\infty}^{X} e^{-X}\left(-\frac{RT^2}{E}\right)dX$ (13)

Replacing $\frac{RT^2}{E}$ with $\frac{E}{RX^2}$ in equation 13,

Then$F(X) = \frac{AE}{\gamma R}\int_{x}^{\infty} e^{-X}\left(\frac{1}{X^2}\right)dX$

$= \frac{AE}{\gamma R}\int_{x}^{\infty} e^{-X}X^{-2}dX$ (14)

Using integral approximation of ref [28],

$\int_{x}^{\infty} e^{-t}t^{-\alpha}dt \approx x^{1-\alpha}e^{-X}\sum_{n=0}^{\infty}\frac{(-1)^n(\alpha)n}{x^{n+1}}$,

equation (14) can be solved as

$F(X) = \frac{AE}{\gamma R}\left[X^{-1}e^{-X}\sum_{n=0}^{\infty}\frac{(-1)^n(2)n}{X^{n+1}}\right]$ (15).

But according to ref [28]

$(\alpha)n = \prod_{k=1}^{n}(\alpha + k - 1)$

= α(α+1)(α+2) . . .(α+n-1)

therefore from (eqn15)

$$(2)n = \prod_{k=1}^{n}(2 + k - 1)$$

$= \prod_{k=1}^{n}(k+1)$

=2(3)(4). . .(n+1)

= (n+1)!

Hence, (2)n in (eqn 15) can be substituted with (n+1)! To obtain

$F(X) = \frac{AE}{\gamma R}\left[X^{-1}e^{-X}\sum_{n=0}^{\infty}\frac{(-1)^n(n+1)!}{X^{n+1}}\right]$ (16)

$= \frac{AE}{\gamma R}\left[X^{-1}e^{-X}\left(\frac{1}{X} - \frac{2!}{X^2} + \frac{3!}{X^3} - \frac{4!}{X^4} + \frac{5!}{X^5} - \frac{6!}{X^6} + \cdots\right)\right]$

$= \frac{AE}{\gamma R}\left[e^{-X}\left(\frac{1}{X^2} - \frac{2!}{X^3} + \frac{3!}{X^4} - \frac{4!}{X^5} + \frac{5!}{X^6} - \frac{6!}{X^7} + \cdots\right)\right]$

$= \frac{AE}{\gamma Rx^2}\left[e^{-X}\left(1 - \frac{2}{X} + \frac{3!}{X^2} - \frac{4!}{X^3} + \frac{5!}{X^4} - \frac{6!}{X^5} + \cdots\right)\right]$

$\approx \frac{AE}{\gamma RX^2}\left[1 - \frac{2}{X}\right]e^{-X}$ (17)

Substituting X and X^2 in equation 17,

$F(T) = \frac{ART^2}{\gamma E}\left[1 - \frac{2RT}{E}\right]e^{-\frac{E}{RT}}$ (18)

Equating 10a and 10b to 17,

We have.

$g(\alpha) = \frac{ART^2}{\gamma E}\left[1 - \frac{2RT}{E}\right]e^{-\frac{E}{RT}}$

Dividing both sides with $T^2$and taking natural log we have

$ln\left[\frac{g(\alpha)}{T^2}\right] = ln\left[\frac{AR}{\gamma E}\left(1 - \frac{2RT}{E}\right)\right] - \frac{E}{RT}$ (19)

Theterm$\frac{2RT}{E}$ is approximately small for the temperature at which most of the reactions take place, therefore equation 19 simplifies to

$ln\left[\frac{g(\alpha)}{T^2}\right] = ln\left[\frac{AR}{\gamma E}\right] - \frac{E}{RT}$ (20)